DCW-R-15-02

NASA Contractor Report 159058

# USER GUIDE FOR STRMLN: A BOUNDARY-LAYER PROGRAM FOR CONTOURED WIND-TUNNEL LINER DESIGN

By

E. Clay Anderson

FINAL SCIENTIFIC REPORT

May 1979

Prepared for

NASA Langley Research Center

Hampton, Virginia 23665

Under Contract NAS1-14517

DCW INDUSTRIES, INC.

4367 Troost Avenue

Studio City, California 91604

TABLE OF CONTENTS

# USER GUIDE FOR STRMLN: A BOUNDARY-LAYER PROGRAM FOR CONTOURED WIND-TUNNEL LINER DESIGN

By
E. Clay Anderson
DCW Industries, Inc.

## SUMMARY

This report is a user guide for a 2-D boundary-layer computer code which was developed in order to process data for an arbitrary number of streamlines. Provisions are included for the computer code to determine either (1) mass transfer rates necessary for an effective boundary-layer displacement of zero thickness or (2) the effective displacement thickness for a specified mass transfer-rate distribution. The computer code has been developed to be compatible with other computer codes which are being modified and/or developed at the NASA-Langley Research Center in order to design the three-dimensional, contoured, wind-tunnel liner to be used in transonic testing of a laminar flow control (LFC) system installed on a supercritical airfoil section.

Appendices to this report present a brief discription of the liner design procedure, representative liner calculations, adaptive-wall design for a two-dimensional wind tunnel test, and other applications.

## INTRODUCTION

The purpose of this report is to provide a user guide for a 2-D boundary-layer analysis computer code (STRMLN) which is

compatible with the string of computer codes being modified and/or developed at the NASA-Langley Research Center in order to design a contoured wind-tunnel liner. The program is written in FORTRAN IV programming language for use on the CDC CYBER series computers at NASA-LRC. A brief description of the current design procedure is given in Appendix A.

Program STRMLN is a modification set for program LTBPG. LTBPG is identical to the program discussed in reference 1 except that LTBPG is restricted to the analysis of perfect gases having a constant or an effective-constant ratio of specific heats. The formulation of the boundary-layer equations and the numerical solution method are discussed in reference 2. In the present report, it is assumed that references 1 and 2 are available, and therefore, only the input data necessary for the present applications are discussed. A number of input paramaters discussed in reference 1 have been assigned values appropriate for two-dimensional flow calculations. One should see reference 1 for the definition of paramaters not given in this report or if program STRMLN is to be applied to other classes of boundary-layer flows.

Representative applications of program STRMLN are presented in appendices B, C, and D. A second modification set for program LTBPG which interacts the boundary-layer displacement with the mean inviscid flow field in nozzles is briefly discussed in appendix E.

## PROGRAM DESCRIPTION

The modification set (STRMLN) has been developed for program LTBPG to analyze the boundary layers along an arbitrary

number of streamlines. The primary purpose of this modification set is to provide the viscous-displacement or the effective-displacement (reference 3) corrections along streamlines defining the contours of a non-porous wind-tunnel liner. The liner is to be used for transonic testing of a laminar flow control (LFC) system on a large-chord yawed-wing model. However, the resulting computer code can be applied without modification to the design of adaptive-wall two-dimensional wind tunnels or other applications where it is necessary to analyze a large number of streamlines. The analysis is restricted to flow fields where the curvature-induced crossflow-velocity components remain small.

For the design of a contoured wind-tunnel liner, more than 200 streamlines may be needed to adaquately describe the liner geometry. This analysis may have to be repeated in order to arrive at a configuration which is compatible with test requirements and constraints imposed by the existing wind-tunnel geometry. Because of the large amount of data to be processed, it is essential that the computer code be relatively free of data manipulation by the user. The present computer code has been applied to representative liner-design calculations and, with the exception of those streamlines where it is necessary to apply suction to avoid flow separation, the data can be processed automatically. For the calculations which have been made to date, there are always a few streamlines at the airfoil/liner junction (both above and below the model) which must be treated individually. The procedure used to define the suction-rate distributions necessary to maintain attached boundary-layer flow requires the user to specify the distribution for each of these streamlines and repeat the procedure until a satisfactory solution is obtained. In order to accelerate this cut-and-try process, the computer code contains logic to permit a number of

suction-rate distributions to be specified for a given streamline. The distributions which result in attached boundary-layer flow are monitored to select the one for output which has the least total mass transferred from the channel. A numerical procedure is being developed to permit the computer code to specify the suction-rate distributions automatically; but, to date, this procedure has not been satisfactory for the abrupt adverse pressure gradients associated with the leading and trailing edges of the airfoil. This procedure provides satisfactory results for relatively gradual adverse pressure gradients but tends to concentrate high levels of suction over a short distance if the pressure gradients are abrupt. The procedure for locating the streamlines for which a flow separation is predicted is discussed in the following paragraphs.

For the present application, the basic liner shape may be considered as rectangular, and data files are generated for each of the four surfaces. These files contain the necessary geometric and pressure coefficient data for approximately 50 streamlines defining each liner surface. The boundary-layer solutions along the streamlines forming the liner walls above and below the airfoil surface can be obtained without difficulty. For the data files containing the streamline data defining the airfoil/liner junction (i.e., the endplates), those streamlines which require suction generally pass within a distance of $\pm 6$ percent chord above and below the junction line, respectively. To determine the number of streamlines which need to be treated individually, one first inspects the inviscid flow-field data and determines the streamline index associated with the streamline which is located approximately 10 percent chord above the airfoil surface. Next a job is submitted to solve the streamlines in sequence up to the previously determined index. Provisions are included within the computer code to monitor the solutions so as to terminate those along streamlines for which flow separation is predicted and advance to the next streamline. Printed messages identiy

the streamlines for which it is necessary to provide suction-rate distributions in order to keep the boundary-layer attached. These streamlines are then computed individually (one for each job submitted) until all streamlines requiring suction have been satisfactorily solved. The remainder of the problem can then be solved without difficulty.

Provisions are also included in the program to permit the analysis of boundary layers on the airfoil surface with options to compute the effective airfoil shape or to compute mass-transfer distributions which result in an effective displacement thickness of zero.

Representative applications of the computer code are presented in appendices B, C, and D. Appendix B summarizes the numerical results obtained for an adaptive two-dimensional wind-tunnel wall shape and presents comparisions with the experimentally determined shape. Applications of STRMLN to the analysis of boundary layers on the airfoil surface are presented in Appendix C. A representative liner calculation is discussed in Appendix D.

## INPUT DATA

Input data to program STRMLN is via punched cards and disc file. The punched card data in namelists and file data are presented in the order which they are read by the program. The namelist name or disc file unit number is given first and is followed by a description of the data read. References to input data not previously defined will be found in a subsequent alphabetical listing. The description of data which is referred to and not defined in the present report is given in reference 1. Many of the input variables which are discussed in reference 1 have been assigned values appropriate for the present application; only those variables which are changed frequently are described herein.

NAMELIST/FIXPT/

IADW - Indicator for thermodynamic condition at wall.

= 0, non-adiabatic
= 1, adiabatic

IBL1 - Subscript in the SS array defining the point where the boundary-layer solution is initiated. Note that for INLT1 $\neq$ 0, SS(IBL1) must have the same value as x read from file NT4.

IBL2 - Subscript in the SS array defining the point where the boundary-layer solution is terminated. Program dimensions require

$$5 \leq IBL2 - IBL1 + 1 \leq 101.$$

ICQZDST - Indicator for mass transfer at wall. If non-zero, the mass transfer distribution for an effective displacement thickness of zero is determined for the interval.

$$SS(IBL1) \leq x \leq SS(IBL2)$$

IE - Number of grid points in the surface normal coordinate used to solve the boundary-layer equations. Maximum permitted value is 101 and is the value normally used.

INLT1 - Indicator. Identifies the record on file NT4 to be used as the boundary-layer starting solution when all streamlines to be solved have the same upstream environment.

JJI - Index which identifies the streamline at which the boundary-layer solutions begin. A value of zero is set to 1.

JJM - Indicator giving the total number of streamlines to be analyzed by the boundary-layer computer code. A value of zero is set to

JJM = JIMAX - JJI + 1

If IMCQD$\neq$0, JJM is assigned a value of 1.

KST2 - Indicator used in conjunction with the output file NT2. A zero value indicates that no previous records have been written on file NT2 and JJI is assigned a value of 1 unless NT2 is assigned a value of 0. If a value of 1 is assigned to KST2 and NT2 is non-zero, records on file NT2 are read up to JJI-1. The data on file NT2 must be recorded in sequential order.

KTRANS - Indicator for boundary-layer transition. If non-zero, a continuous transition from laminar to turbulent flow is computed. LAMTRB is set to 1 and CHICRT must be defined.

KTRNSN - Subscript in XSTA array defining the point at which the boundary-layer is assumed to make the transition from laminar to turbulent flow instantaneously. A value of 0 is set to IBL2-IBL1 + 1. If a non-zero value is input, LAMTRB is set to 1.

LAMTRB - Indicator for type of boundary layer.

= 1 for laminar or transitional flows.
= 2 for turbulent flow.

Note that KTRANS or KTRNSN $\neq$ 0, must have LAMTRB = 1.

NASY - Indicator for previous file processing by assembly program. 0 indicates that the input data file (NT1) has not been processed by the assembler program (see Appendix A). A value of 1 indicates input data has been processed by assembler program.

NT1 - Unit number for streamline data input file.

NT2 - Unit number for streamline data output file.

NT3 - Unit number for auxiliary output file.

NT4 - Unit number for boundary-layer starting solution input data file.

Note: NT1 must be defined. NT2, NT3, and NT4 are bypassed if assigned a value of zero.

NAMELIST/FLTPT/

BO - If IADW is 0, the surface temperature is held constant at the value BO*TSTAG.

CHICRT - Vorticity Reynolds number at which a continuous transition from laminar to turbulent flow is initiated. KTRANS must be non-zero for a continuous transition, and KTRNSN is assigned a value of 0. The normal range for the critical vorticity Reynolds number at the transition point is

$$2000 \leq \text{CHICRT} \leq 4000$$

for subsonic 2-D flows. If KTRANS is non-zero and CHICRT is 0, transition is initiated at a momentum thickness Reynolds number of 1000.

CHORDWN - Chord length (in feet) measured in the wing-normal direction (i.e. normal to the leading edge of a yawed wing).

DX - Initial streamwise integration stepsize.

DXMAX - Maximum streamwise integration stepsize permitted.

G - Ratio of specific heats.

PRL - Molecular Prandtl number. A value of 0 is set to 0.7.

PRT - Turbulent Prandtl number. A value of 0 is set to 0.9.

PSTAG - Stagnation pressure, PSIA.

RECHSTL - Reynolds number based on the streamwise chord length. The value is input as 0 and is computed by the computer program.

RECHWN - Reynolds number based on the wing-normal chord length. The value is input as 0 and is computed by the computer program.

TSTAG - Stagnation temperature in degrees Rankine.

NAMELIST/MASSTR/

ICQD - A non-zero value indicates that the mass transfer rate distribution changes discontinuously. Up to 10 discontinuous changes in the mass transfer rate can be entered in the array CQD.

IMCQD - If non-zero, the streamline JJI is solved any desired number of times using different mass-transfer rate distributions. The present namelist is read after each solution is obtained, and the solutions are terminated when an end-of-file is read.

IMT - If non-zero, a mass transfer rate distribution or distributions must be specified.

KEMT - Array of subscripts for the XSTA array (see reference 1) indicating the points where mass transfer is terminated or changes discontinuously. KEMT is dimensioned for 10 values. A shifted index is used to define the XSTA array and is defined as follows:

$$XSTA(N) = SS(K)$$

where

$$N = K - IBL1 + 1$$

and

$$IBL1 \leq K \leq IBL2$$

KIMT - Array of subscripts in the XSTA array (see reference 1) defining the points where mass transfer is initiated or changes discontinuously from one level to another. KIMT is dimensioned for 10 discontinuous changes in the mass transfer rate. If ICQD is non-zero, the array CQD must have the same number of entries as the arrays KIMT and KEMT. If the mass transfer rate distribution has a continuous variation, only 1 value of KIMT and KEMT are entered, and the mass transfer rate distribution CQS must be entered at all points in the XSTA array. Note that CQS can change from 0 to a finite value or from a finite value to 0 at the points where mass transfer is initiated or terminated.

CQD - Array of mass transfer rates which change discontinuously from one level to another at the beginning of intervals defined by KIMT and KEMT. ICQD must be non-zero and the same number of entries must be made for KIMT, KEMT, and CQD. CQD is dimensioned by 10.

CQS - Array of mass transfer rates which have a continuous variation in the interval KIMT (1) to KEMT (1). Outside this interval the values of CQS must be entered as zeros. The number of entries in the CQS array is IBL2-IBL1 + 1 $\leq$ 101.

DISC FILE INPUT DATA. UNIT NT1.

The disc file input data contains a number of variables which are not used in the boundary-layer computer code. These data have been used in previous processing steps or will be used in the post processing step. A description of all input data is given, and the data which is necessary for the boundary-layer

calculations are superscripted with an asterisk (*). In the description of the disc file input data, the records and the variable names are presented in the order in which they are read, and the format is given. The variable names are then defined in alphabetical order following each record.

DESC2 (8A10)

DESC2, Alphanumeric description data identifying one previous processing procedure.

DESC1 (8A10)

DESC1, Alphanumeric description data identifying one previous processing procedure.

DESC3 (8A10) (Read only if NASY = 1)

DESC3, Alphanumeric description data identifying previous processing procedure.

AMIN, QIN, ALAMD, AMI*, QI, CPST (8E16.8)

ALAMD - Sweep angle in degrees.

AMI* - Freestream Mach number.

AMIN - Component of freestream Mach number normal to the wing leading edge.

CPST - Pressure coefficient at sonic condition.

QI - Freestream velocity, feet per second.

QIN - Freestream velocity component normal to the wing leading edge, feet per second.

IMAX*, ILE*, ITE*, JIMAX*, JIL*, JJU*, (16I5)

ILE* - Subscript in the SS array identifying the location of wing leading edge. For boundary-layer calculations on the airfoil surface JJI is input as JIL or JIU; IBL1 = ILE-1; IBL2 = ITE-1; NT2 = 0; and JJM is either 1 or 2.

IMAX* - Related to the number of data points in the SS array. IMAX is used by the programs generating the streamline data and two of the data points are not recorded on the input file.

The boundary-layer computer code uses IMAX1 = IMAX-2 and is dimensioned for $5 \leq$ IMAX1 $\leq 101$.

ITE* - Subscript in the SS array identifying the location of the wing trailing edge.

JIMAX* - Number of streamline records written on this disc file.

JIL* - Index identifying the streamline associated with the airfoil lower surface.

JIU* - Index identifying the streamline associated with the airfoil upper surface. Note ahead of and behind the airfoil, the y-values associated with these two indices are the same.

ALSBD, ALSTD, YJSB, YJST, SPAN, YSTLC (8E16.8) (Read only if NASY = 1)

These quantities are not used by program STRMLN. These are parameters pertaining to the assembly of streamline data into either a "flat" end plate (wall) or an "octagonal" endplate (wall). They must be read and transferred through this program for use later in the processing step.

JSB, JST (16I5) (Read only if NASY = 1)
Above remarks apply to these quantities also.

XS(N), YS(N), ZS(N), CPS*(N), SS*(N), DSTREF*(N), (8E16.8) N = 1, IMAX1 (8E16.8)

CPS* - Pressure coefficient on streamline.

DSTREF* - Effective displacement thickness normalized with respect to the wing-normal chord length. Input as zero to initialize the array.

SS* - Distance along the streamline normalized with respect to the wing normal chord length.

XS,YS,&ZS - Cartesian coordinates of streamlines defining the inviscid liner contours. The coordinates are normalized with respect to the wing-normal chord length. These coordinates are corrected for the displacement effect in the post processing step.

DISC FILE INPUT DATA. UNIT NT4.

Input data file NT4 is used if all streamlines to be solved have the same upstream environment. The boundary-layer starting solution data written on unit NT4 is generated using program LTBPG.

INLT - (Unformatted)

INLT - Record index used in conjunction with INTL1 to select the desired boundary-layer starting solution.

X, XI, Z, ZØL, RO, BETA, PP, NIT, K, TE, UE, XM, RØWE, XMUE, PE, DUEDS, CF, QW, HG, EPSVD, DM, KEP, NITTØT, CHIMAX, GAMMA, XIBAR, REX, QDØT, HG1, HG2, STE, STINF, CHEDGE, CH, CHREY, HAFCF, CHØCF, XØREFL, ZØREFL, RØREFL, DELØX, THØREF, DSTØRF, DSAXØR, THØDEL, DSTØDL, DSTØTH, DSTRAX, DSTARK, DELST, DEL, THET, RETHET, XN, YY, YØVTHT, FC, FCN, F2NN, EPSPL, A0BP, TC, TCN, TH, RØRØE, C, CP, CHI, ETAINF, PNC, DS, XIØLD, XØLD, UERO2, RØWEP, XMUEP, CFI, AIB, Y, FCP, THP, DN, F1, F1N, F1NN, F2, F2N, T1, T1W, T1NN, T2, T2N, T2NN.- (Unformatted)
Definitions of the variables appearing in this record are given in reference 1.

## OUTPUT DATA

Output data from program STRMLN is via printed computer forms and disc files. The printed output is primarily a listing of some of the input data, those boundary-layer results needed for determining mass-transfer distributions along individual streamlines and error messages. The disc file output is the information which is transferred to the post processing step in order to make a wall correction for the effective displacement thickness.

PRINTED OUTPUT

The printed output provides only a minimum amount of information. The previously defined input is listed first and is followed by a listing of the geometric coordinates and edge conditions for the first streamline to be solved. Geometric coordinates and edge conditions for subsequent streamlines are not listed. Solution data for each streamline consist of a listing of the surface mass-transfer rate (if applied), displacement-thickness, and effective displacement-thickness (if surface mass transfer is applied) distributions. These data are followed by a message identifying the streamline.

DISC FILE OUTPUT DATA. UNIT NT2.

Unless specified, all data written on the output file have been previously defined, and only the variable names and the format for each record is given.

INFØ(1), INFØ(23), INFØ(22) (YSTLTB*, A7, 2X, 2A10*, from program STRMLN*)

INFØ - Processing data retrieved from the computer operating system when the job is first submitted. INFØ(1) is the job name assigned by the operating system, - INFØ(23) is the date, and INFØ(22) is the time of execution. This information is put on the file by every program which processes it.

DESC2 - (8A10)

DESC1 - (8A10)

DESC3 - (8A10), written only if NASY = 1.

AMIN, QIN, ALAMD, AMI, QI, CPST (8E16.8)

IMAX, ILE, ITE, JIMAX, JIL, JIU (16I5)

ALSBD, ALSTD, YJSB, YJST, SPAN, YSTLC (8E16.8)(written only if NASY = 1)

JSB, JST (1615) (written only if NASY = 1)

BO, CHØRDWN, PSTAG, RECHWN, RECHSTL, TSTAG (8E16.8)
IADW, IBL1, IBL2, JJI, JJM, KTRANS, KTRNSN, LAMTRB (16I5)

The 10 records listed above are written only when the job is first submitted.
XS(N), YS(N), ZS(N), CPS(N), SS(N), DSTREF(N), N =1, IMAX1
(8E16.8)

AUXILIARY DISC FILE OUTPUT DATA. UNIT NT3.

The auxiliary output file is used for plotting purposes only, and the data written is variable.

## APPENDIX A

## OUTLINE OF THREE-DIMENSIONAL WIND TUNNEL LINER DESIGN PROCEDURE FOR THE NASA LFC EXPERIMENT

Currently available inviscid transonic and boundary-layer analysis computer codes are being modified at the NASA-Langley Research Center in order to design a non-porous wind-tunnel liner for the purpose of testing a laminar flow control (LFC) suction system installed on a super-critical airfoil section. The proposed test is to be conducted in the Langley 8-foot transonic pressure tunnel at a freestream Mach number of 0.82. The streamwise model-chord length of 7 feet results in a very small tunnel height-to-chord ratio. This experiment and test facility are being designed to simulate free-air flow about an infinite aspect-ratio yawed wing, so that two-dimensional design and analysis methods are applicable. For this case, the three-dimensional flow field is obtained by the addition of a constant crossflow-velocity component to the two-dimensional flow-field solution obtained for the airfoil at the appropriate reduced freestream Mach number. The streamlines (particle paths) forming the liner contours in the test section are to be determined from this velocity field. In order to make a smooth connection with the existing tunnel upstream of the contoured test section, the liner contour is obtained by superimposing the three-dimensional airfoil (yawed wing) flow-field perturbation onto the velocity field of an appropriate wind-tunnel contraction section.

The sensitivity of high-speed channel flows to minor variations in the effective area-ratio distribution requires that viscous-displacement corrections be made to the inviscid liner contours. A two-dimensional boundary-layer analysis is appropriate for all streamlines forming the liner contour except those near the airfoil/liner junction, since outside of this region, the streamline curvature induced crossflow velocity components along the

liner walls are negligible. The flow in the immediate vicinity of the airfoil/liner junction is three-dimensional and is to be controlled by applying variable suction rates on both the liner wall and the airfoil surface.

The departure from conventional test procedures results in part from the necessity to (1) use a relatively large-chord model in order to provide adequate space for the LFC suction system, (2) satisfy Reynolds number scaling requirements, and (3) conduct the test in a quiet, low-turbulence transonic wind tunnel. For conventional testing at super-critical speeds, a wind tunnel height-to-chord ratio of 3 to 4 is necessary (see reference 4) to avoid excessive tunnel induced interference effects. In principal, the contoured-liner concept permits the use of tunnel height-to-chord ratios of any size. However, at super-critical flow conditions, the liner is restricted in its application to a specified test model at a specified test condition and permits only limited variations in test conditions about the design point.

There are four basic tasks in the contoured liner design procedure and each of these tasks is accomplished by several computer codes which pass information along on disc files. These tasks are:

(1) inviscid yawed-wing test-section design;
(2) inviscid 3-D contraction design;
(3) viscous displacement correction; and
(4) post processing of data.

In the following paragraphs, a brief description of each task in the liner design procedure is presented.

INVISCID YAWED-WING TEST-SECTION DESIGN

The airfoil ordinates which produce a specified set of performance characteristics at the design Mach number are determined using

the NYU fast-solver computer code developed by Bauer, Garabedian, Korn, and Jameson, reference 5. The flow-field solution determined by this analysis is given in a transformed coordinate system, and the liner design procedure requires the flow-field properties and geometric data to be expressed in a Cartesian coordinate system. This could be obtained by an inverse transformaion of the coordinate system used in reference 5. A more convenient procedure, however, is to recompute the flow field about the previously determined airfoil configuration using the TRANDES computer code developed by Carlson, reference 6, which determines the flow-field solution in the required coordinate system.

The yawed-wing streamlines are determined by integration of the 2-D velocity components (i.e., those lying in a plane perpendicular to the wing leading edge) and the constant orthogonal sweep-velocity component. This 2-D integration starts from an initial set of ordinates well upstream of the airfoil and ends far downstream from it. A streamline assembly program forms the liner by translating these space curves according to sweep theory. The final program in this step interpolates these assembled curves onto a grid which is fixed in the tunnel in order to define the ordinates for starting the upstream integration through the contraction section, draw pictures of the test section lines, and perform other appropriate data processing.

INVISCID 3-D CONTRACTION DESIGN

To define the coordinates of the wind tunnel liner surfaces in the contraction section, it is necessary to superimpose the perturbation velocity field due to the yawed-wing onto the velocities for an axially-symmetric contraction which far upstream can be related to the existing tunnel. The streamline

analysis is made using the General Electric computer code STC (reference 7). To provide the necessary data for superimposing velocities and then integrating upstream, the outer boundaries of the approximate contraction must extend outside the boundaries of the existing wind-tunnel facility. The streamtube which closely approximates the far upstream area of the existing tunnel must closely approximate the area of the three-dimensional liner at the match point in order to conserve mass. An iterative process is necessary to arrive at an approximate configuration which satisfies the requirements of the liner design in the test section and which contains the approximate streamtube that can be fitted within the boundaries of the existing wind tunnel.

The velocity field for this axi-symmetric nozzle solution is interpolated onto a cartesian grid and then a velocity perturbation due to flow about the yawed-wing model is superimposed. This produces a 3-D velocity field on a cartesian grid in the contraction section region. A 3-D integration upstream through this velocity-field gives shapes which are taken to be the inviscid 3-D contraction section. At the far upstream end, where the Mach number is low, these lines are faired back into the existing tunnel.

VISCOUS DISPLACEMENT CORRECTIONS

The coordinates defining the physical liner surfaces are the inviscid liner coordinates plus the viscous displacement correction or the effective displacement correction (reference 3) if surface mass transfer is applied along streamlines. The displacement corrections to the inviscid streamline coordinates and the suction rates necessary to maintain an attached boundary-layer flow are determined using program STRMLN discussed in this report. If the displaced geometric coordinates of the

liner surface fall outside the existing wind-tunnel boundaries, it is necessary to repeat some aspects of the two design tasks outlined above. Since the lines are faired into the existing tunnel far upstream, an approximate starting solution for the boundary layer is required. It is obtained from LTBPG.

POST PROCESSING OF DATA

The final step in the liner design procedure is to process the data to put it in a format suitable for engineering and fabrication purposes. The liner shapes are given as parametric space curves and need to be interpolated onto a suitable reference system showing elevation, cross-sections, etc.

It can be seen that tasks 1 and 3 above are applicable to the design of adaptive wall two-dimensional wind tunnels. Results for such an application and comparison with the experimentally determined shape are given in Appendix B.

# APPENDIX B

## APPLICATION OF STRMLN CODE IN 2-D ADAPTIVE-WALL WIND-TUNNEL DESIGN

The numerical procedure being developed for contoured wind-tunnel liner design (see appendix A) has been applied to define the wall shape for a two-dimensional adaptive-wall wind-tunnel test. The numerically determined wall shape is compared with the wall shape determined by Barnwell and Everhart* using an iterative analytical/experimental method. Complete details of this application are presented in reference 8, and only a summary of the results are presented here.

The experimental data were obtained in the NASA Langley 6- by 19-Inch Transonic Tunnel (reference 9). For this experiment, the slotted wind-tunnel walls were removed and replaced by nonporous flexible jack-supported plates as shown in figure B-1. The model used is an NACA-0012 symmetric airfoil section at zero incidence and the test conditions were:

Freestream Mach number, $M_\infty = 0.765$
Freestream Reynolds number, $N_{Re,\infty} = 2.00 \times 10^5$/cm
Stagnation pressure, $P_0 = 1.42 \times 10^5$ Pa
Stagnation temperature, $T_0 = 282\ ^\circ K$

The chord length, c, is 15.24 cm (6 inches) and the model was centered at the ⊕ mark shown in figure B-1. Coordinates x/c and y/c are measured along and perpendicular to the wind tunnel's horizontal plane of symmetry with origins at the center mark and the plane of symmetry, respectively.

---

*A detailed description of the streamline procedure and results obtained from it have not yet been published by R. W. Barnwell and J.L. Everhart of NASA Langley Research Center. The present analytical results are compared with their experimentally determined wall shape; we appreciate and acknowledge this early release of their data. In this paper their procedure and results will be identified as Barnwell-Everhart.

NASA LANGLEY 6- BY 19-INCH TRANSONIC TUNNEL
WITH SLOTTED WALLS REPLACED BY FLEXIBLE WALLS

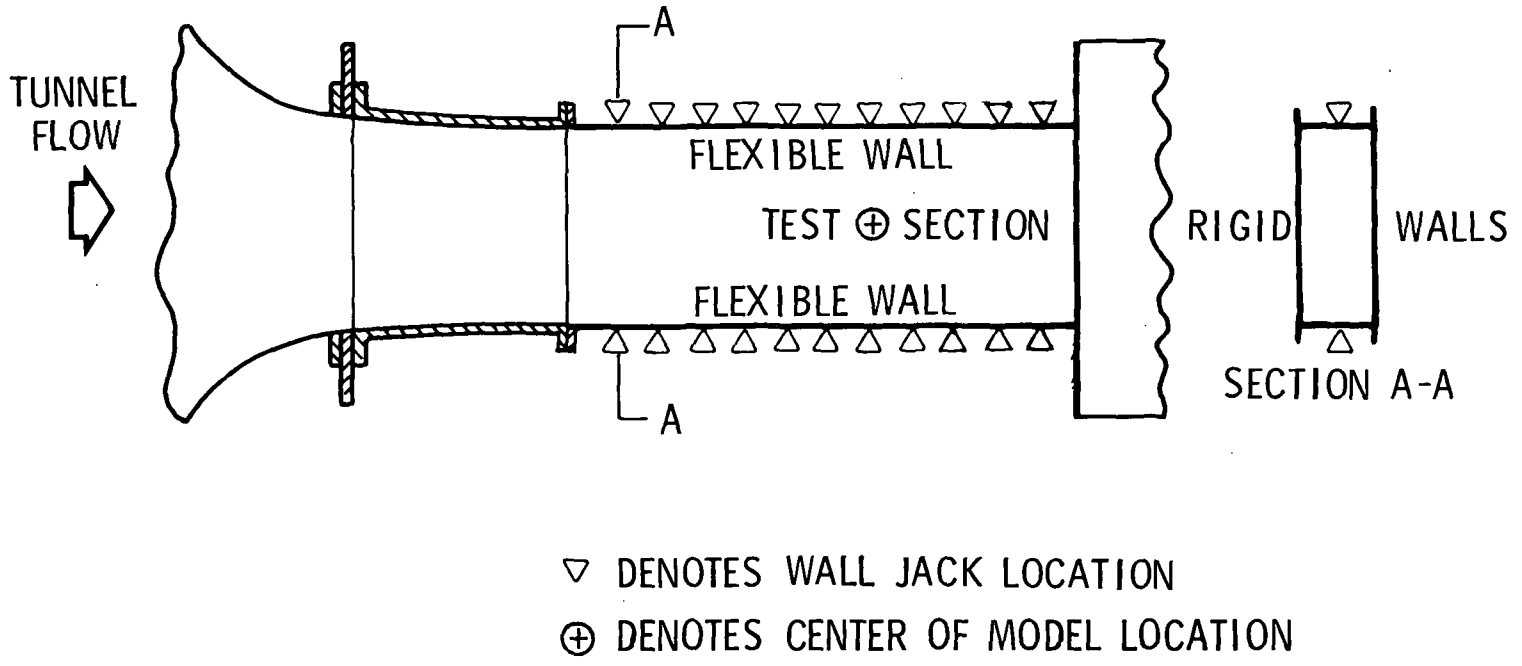


Figure B-1.- Schematic of two-dimensional "streamlined tunnel" experiment of Barnwell and Everhart.

The free-air solution about the airfoil geometry plus the viscous displacement correction were determined using the transonic design/analysis computer code discussed in reference 5 and the transonic analysis computer code presented in reference 6. At the upstream junction of the flexible and rigid tunnel walls ($x/c = -4.833$), 48 streamlines lying in the region $0 \leq y/c \leq 1.583$ were extracted from the free-air solution for boundary-layer calculations. The starting boundary-layer solution was taken as that for a two-dimensional model of the wind-tunnel geometry up to the junction of the flexible and rigid tunnel walls. From this starting solution, boundary-layer calculations were made along each of the streamlines to define the viscous-displacement thickness distributions. The two-dimensional boundary-layer equations cannot be integrated into the strong adverse pressure gradients associated with the streamlines near the airfoil/tunnel junction; it was necessary to make modifications to the pressure distributions in the vicinity of the airfoil leading edge. The procedure used in the analysis was to replace four values of the pressure coefficient along each of four streamlines lying within the region $-0.57 \leq x/c \leq -0.49$ by the corresponding values associated with the first streamline for which the boundary-layer analysis did not predict a flow separation. This in effect reduces the pressure gradients to a value slightly below that for a predicted boundary-layer separation. More drastic changes in the pressure coefficients than those used in the analysis had a negligible effect upon the solutions downstream of the leading edge. However, this procedure should not be used if the zone of the separation extends to an appreciable part of the sidewall. All of the modified streamlines are close to the airfoil/tunnel-sidewall junction where the flow is three-dimensional and the present analysis is not expected to be very accurate either with or without the modifications in this region.

Figure B-2 presents boundary-layer displacement-thickness distributions across the tunnel sidewall (or across streamlines) at six locations along the streamwise direction. In the region $-2.10 \leq x/c \leq -0.57$, the distributions show the expected upstream influence of the model pressure field. The plot at $x/c = -0.57$ shows the influence of a favorable pressure gradient upon the sidewall streamline far from the model. That is, the displacement thickness along these outer streamlines at this location are less than those at an upstream location. The inflection point in the displacement-thickness distribution at $x/c = -0.31$ is the result of different flow acceleration rates along the streamlines and a difference in distance measured along the streamlines relative to their respective upstream pressure peaks. The termination point of this plot above the y/c-origin represents the airfoil thickness at this location.

Displacement thickness distributions at $x/c = 0.506$ and 1.07 show the influence of the trailing-edge compression and a representative downstream profile. The inflection point in the displacement thickness distributions at $x/c = 1.07$ is the result of the more rapid flow acceleration along streamlines near the corner of the (effective inviscid) blunt trailing edge of the airfoil.

As shown in figure B-1, only the two lateral walls opposite the airfoil surfaces are flexible. Thus, at each streamwise location, x/c, the displacement thickness, $\delta^*/c$ (x/c, y/c), must be integrated around the local cross-sectional perimeter and then be applied as a displacement of only the two lateral flexible walls. Since no displacement correction was made at the (upstream) junction of the fixed rigid wall and the flexible plates, the wall displacement correction is made relative (differential) to that at this junction. The total wall displacement is composed of two components: (1) the departure of

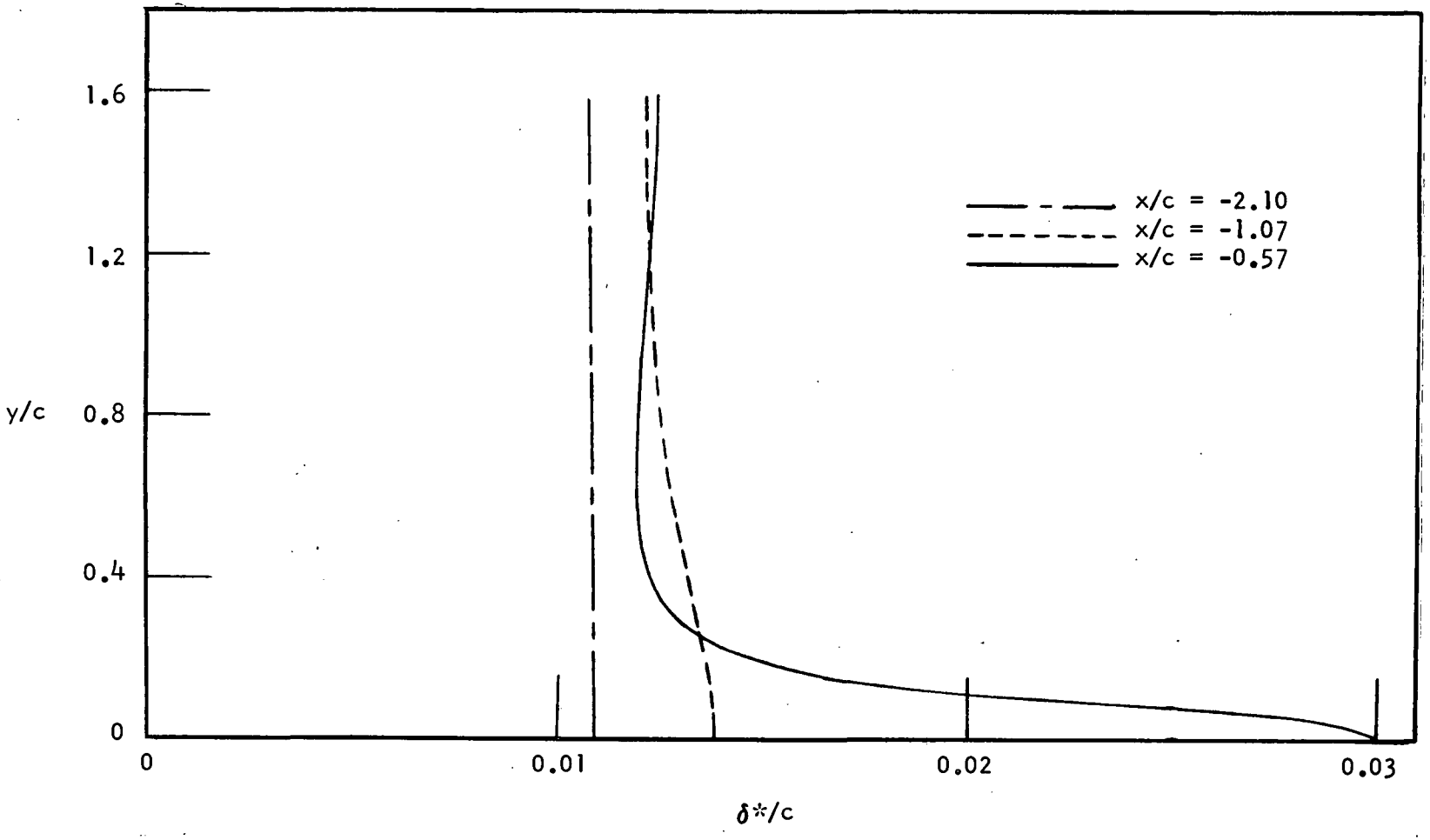


Figure B-2a. Calculated boundary layer displacement thickness distributions on the tunnel sidewall across six lateral cuts.

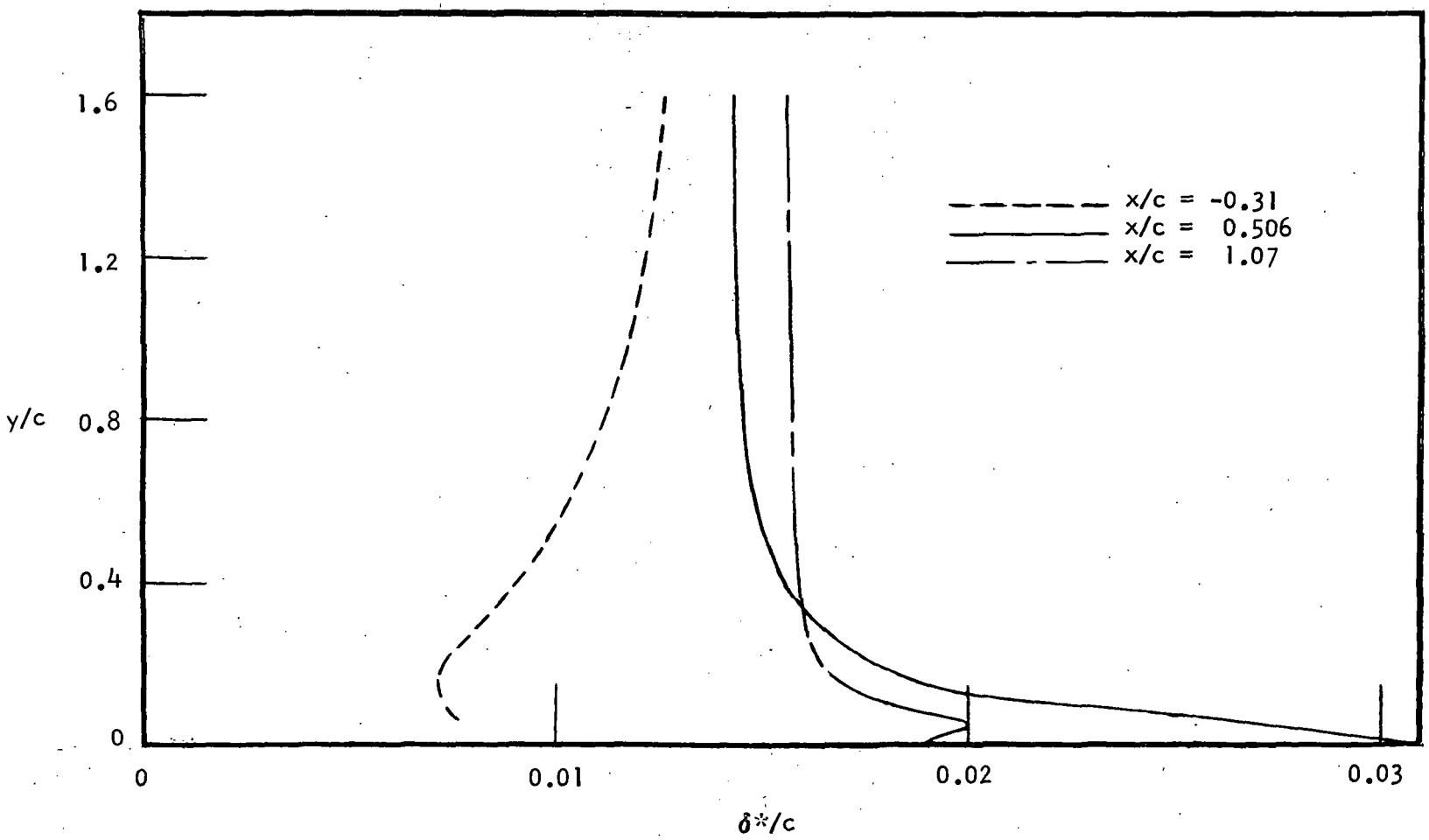


Figure B-2b.- Concluded.

the outer bounding streamline from a straight line - the compressible blockage correction and (2) the boundary-layer displacement on all of the wind-tunnel walls - the viscous blockage correction. Comparisons of the numerically determined wall shapes with the experimental data of Barnwell and Everhart are shown in figure B-3. The symbols show the total experimentally determined displacement at the 11 jack-point locations indicated in figure B-1. The maximum difference between the analytically-determined wall-displacement corrections and the experimental data is at $x/c = -0.667$. At this location, the displacement corrections differ by less than 8 percent and the ratio of the two coordinates, which indicates the difference in the tunnel area ratio, is 1.002. The displacement contributed by the deflection of the outer bounding free-air streamline is also shown in the figure.

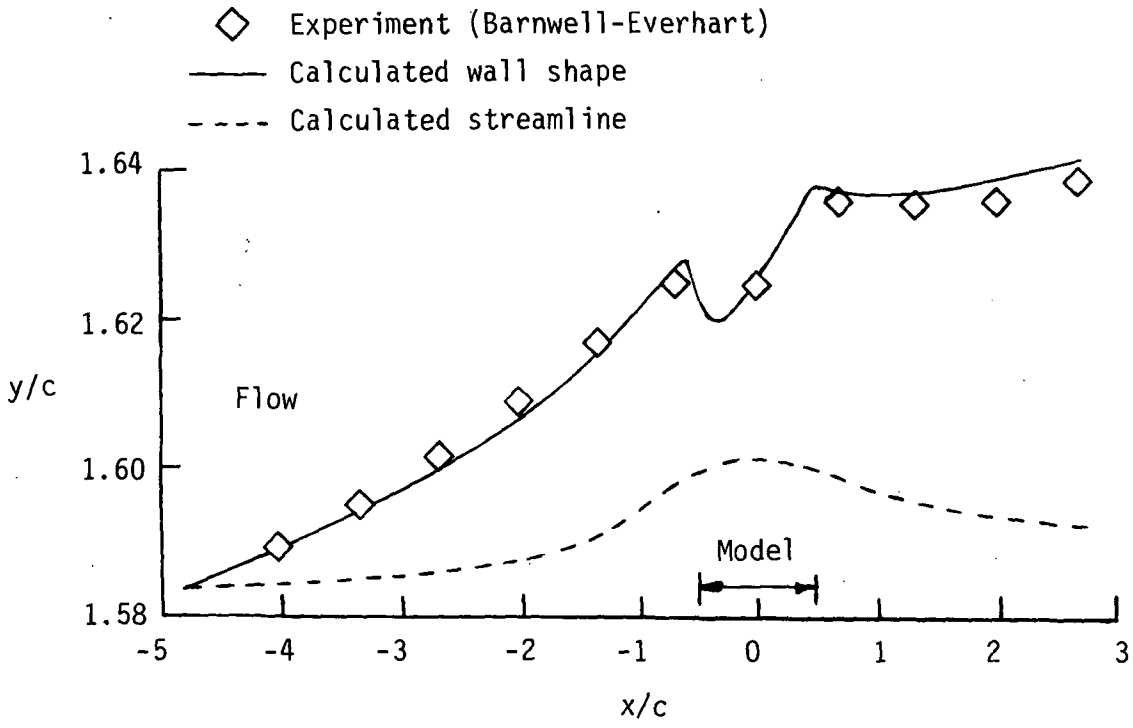


Figure B-3. Comparison of flexible nonporous wall shapes for an NACA 0012 airfoil test at zero lift in the Langley 6- by 19-inch transonic tunnel.

## APPENDIX C

## APPLICATION OF STRMLN CODE TO ANALYSIS OF SUCTION ON AN LFC AIRFOIL

Surface mass-transfer rate distributions required to maintain laminar flow on an LFC airfoil designated as YNRB-12-2-77 (Reference 10) have been determined using a laminar-flow stability analysis. The present two-dimensional computer code has been used to determine the effective displacement-thickness distributions on the airfoil surface. The effective displacement thickness, $\Delta^*/c$, is defined as (see Reference 3):

$$\Delta^*/c = \delta^*/c + \frac{1}{\rho_e u_e} \int_0^X CQ(x/c)\, d(x/c) \qquad (1)$$

where

$$\delta^*/c = \int_0^\infty \left[ 1 - \frac{\rho u}{\rho_e u_e} \right] d(y/c) \qquad (2)$$

In these expressions, $\rho u$ and $\rho_e u_e$ are the tangential mass fluxes at a local point and at the boundary-layer edge, respectively; and $CQ(x/c)$ is the surface mass-transfer rate distribution normalized with respect to the freestream mass flux. (See Reference 1.)

The assumed test conditions for this LFC airfoil calculation are as follows:

Freestream Mach number, $M_\infty = 0.891$
Freestream Reynolds number, $N_{Re,\infty} = 15 \times 10^6$, based on the streamwise chord
Stagnation pressure, $P_o = 5.87$ PSIA
Stagnation temperature, $T_o = 508^\circ$ R
Wing-Normal chord, $c = 6.553$ ft.

Streamwise chord, $\hat{c}$ = 8.0 ft.
Sweep angle, $\Lambda$ = 35°

The airfoil ordinates and surface pressure distributions are shown in figure C-1 and the surface mass transfer rates are shown in figure C-2. Figure C-3 presents the corresponding effective displacement thickness distributions for laminar flow. The effective displacement thickness is negative over approximately 80 percent of the chord on the lower surface and over approximately 25 percent of the chord on the upper surface. The effective displacements for this case are not large enough to result in a significant change in the airfoil pressure distribution; however, in order to check the steps in the design procedure, the displacement thickness was added to the airfoil ordinates, and the free-air flow field about the effective airfoil geometry was recomputed using the transonic analysis computer code discussed in reference 5. Figure C-4 presents a comparison of the pressure distributions and sonic line locations for the airfoil ordinates and the effective airfoil ordinates.

On the outboard portions of the airfoil model, the turbulent liner-wall boundary layer will contaminate the flow over the airfoil surface and result in turbulent zones of flow. To determine the effective turbulent displacement-thickness distributions in flow regions where the laminar-stability mass-transfer rates are applied, the boundary layer was assumed to be fully turbulent, and the resulting effective displacement-thickness distributions are shown in figure C-5. These turbulent $\Delta^*/c$'s are sufficiently large to significantly alter the airfoil pressure distribution. This influence can be controlled by subtracting the effective displacements from the airfoil ordinates but would result in a compound airfoil surface. An

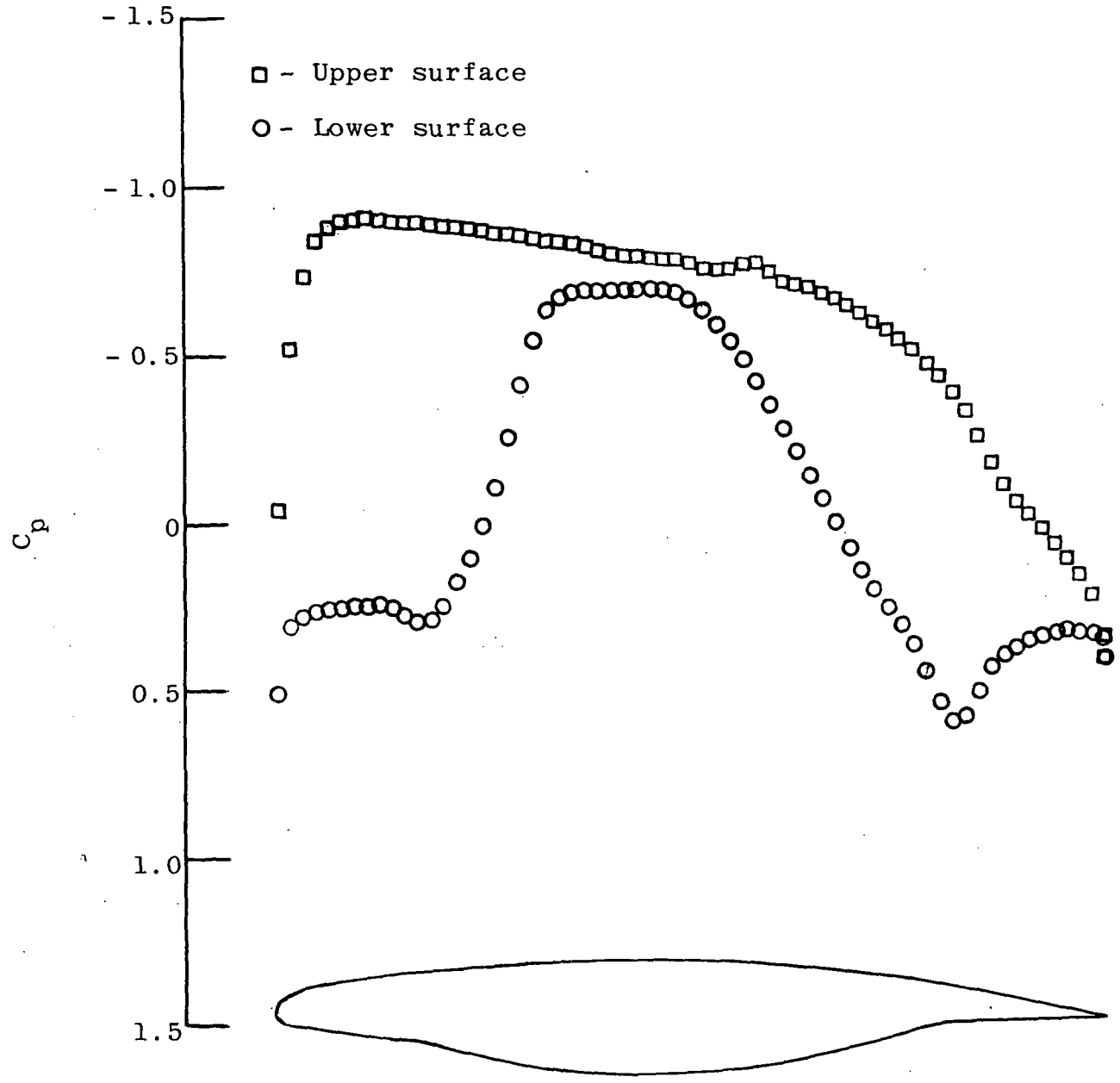


Figure C-1.- 2-D pressure coefficient distributions and coordinates for LFC Airfoil YNRB-12-2-77.

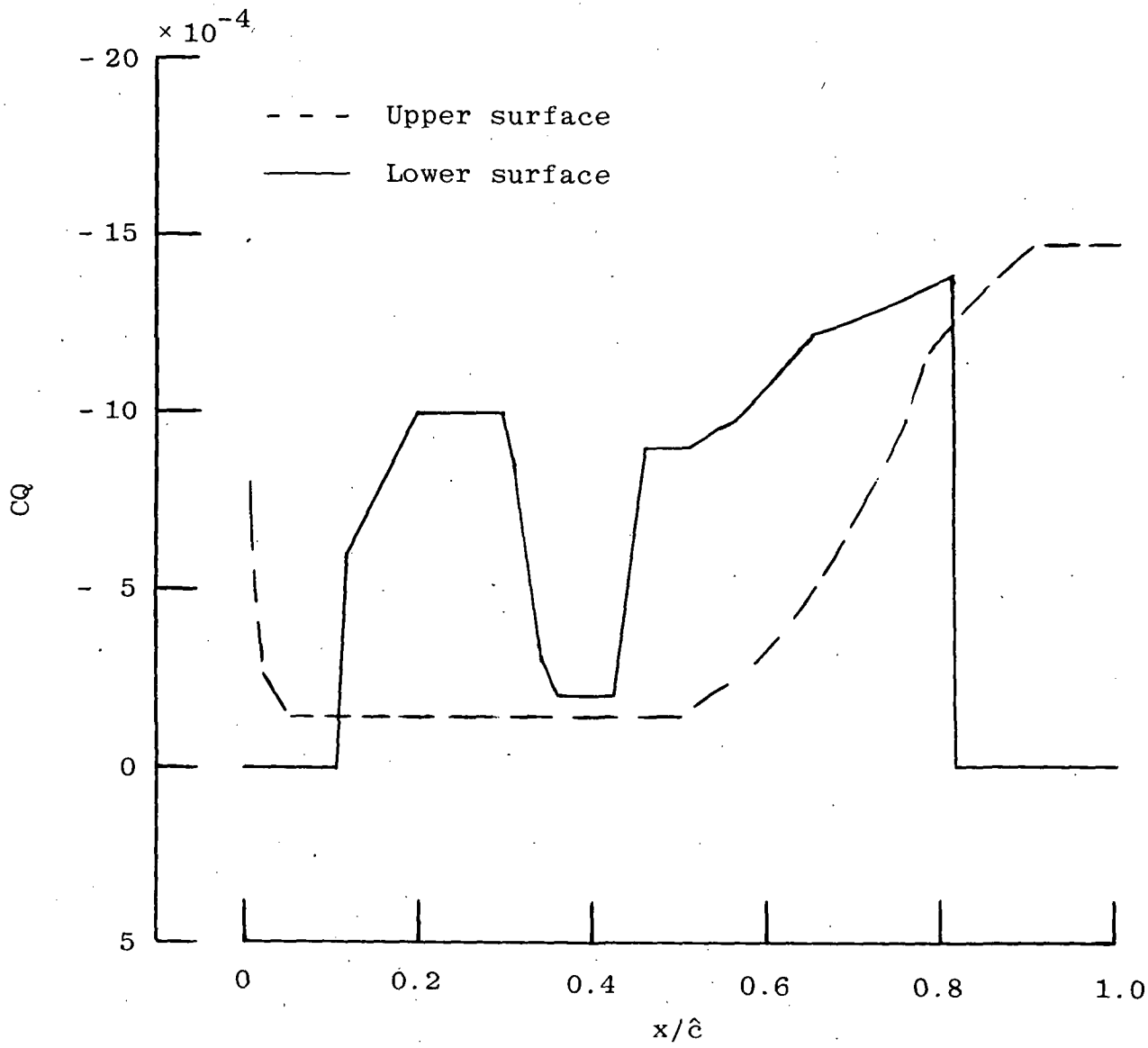


Figure C-2.- Surface mass-transfer rate distributions for laminar flow stability on LFC Airfoil YNRB-12-2-77 at test conditions.

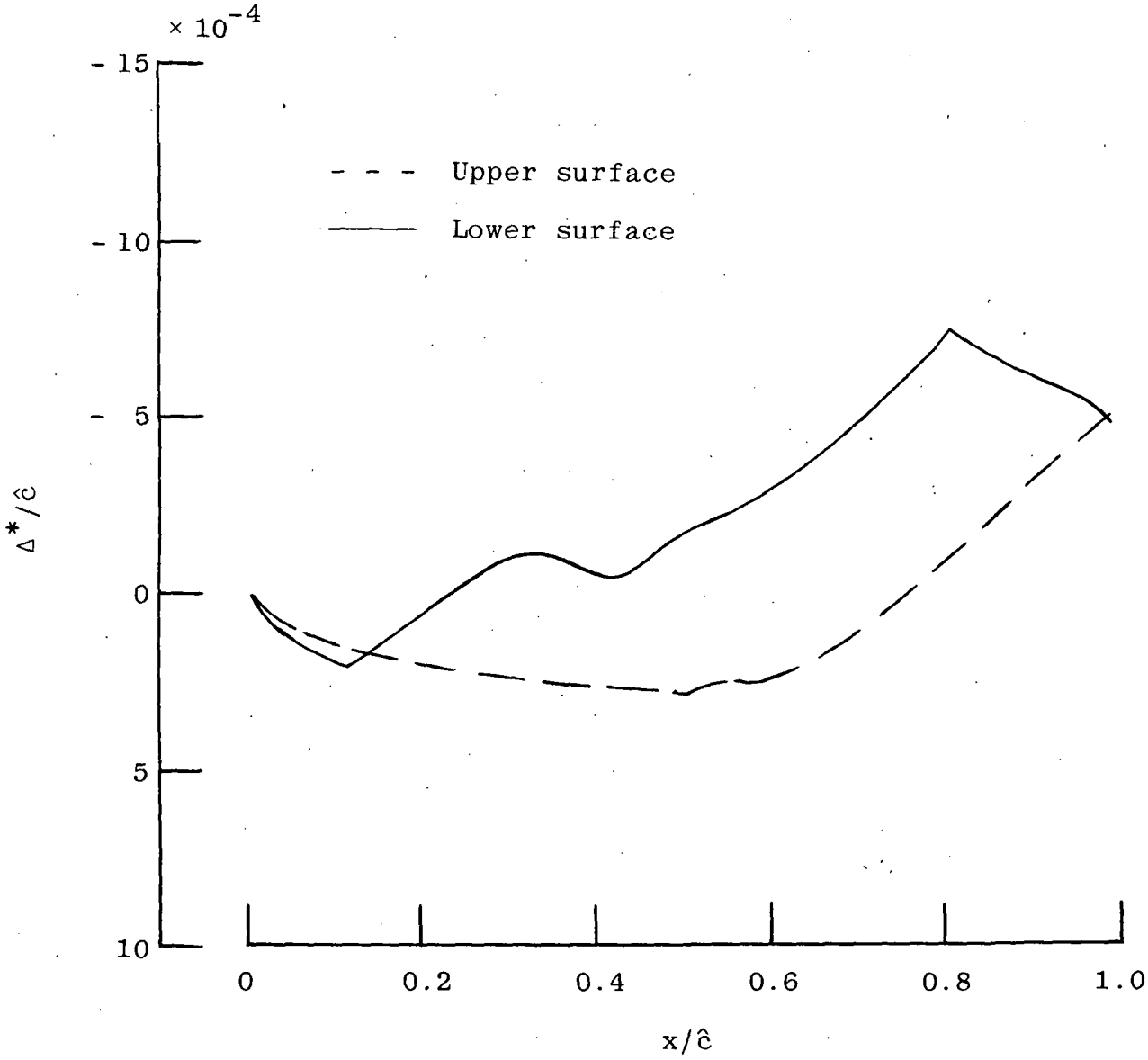


Figure C-3.- Effective displacement-thickness distributions for laminar flow with laminar flow stability suction rates applied on LFC Airfoil YNRB-12-2-77 at test conditions.

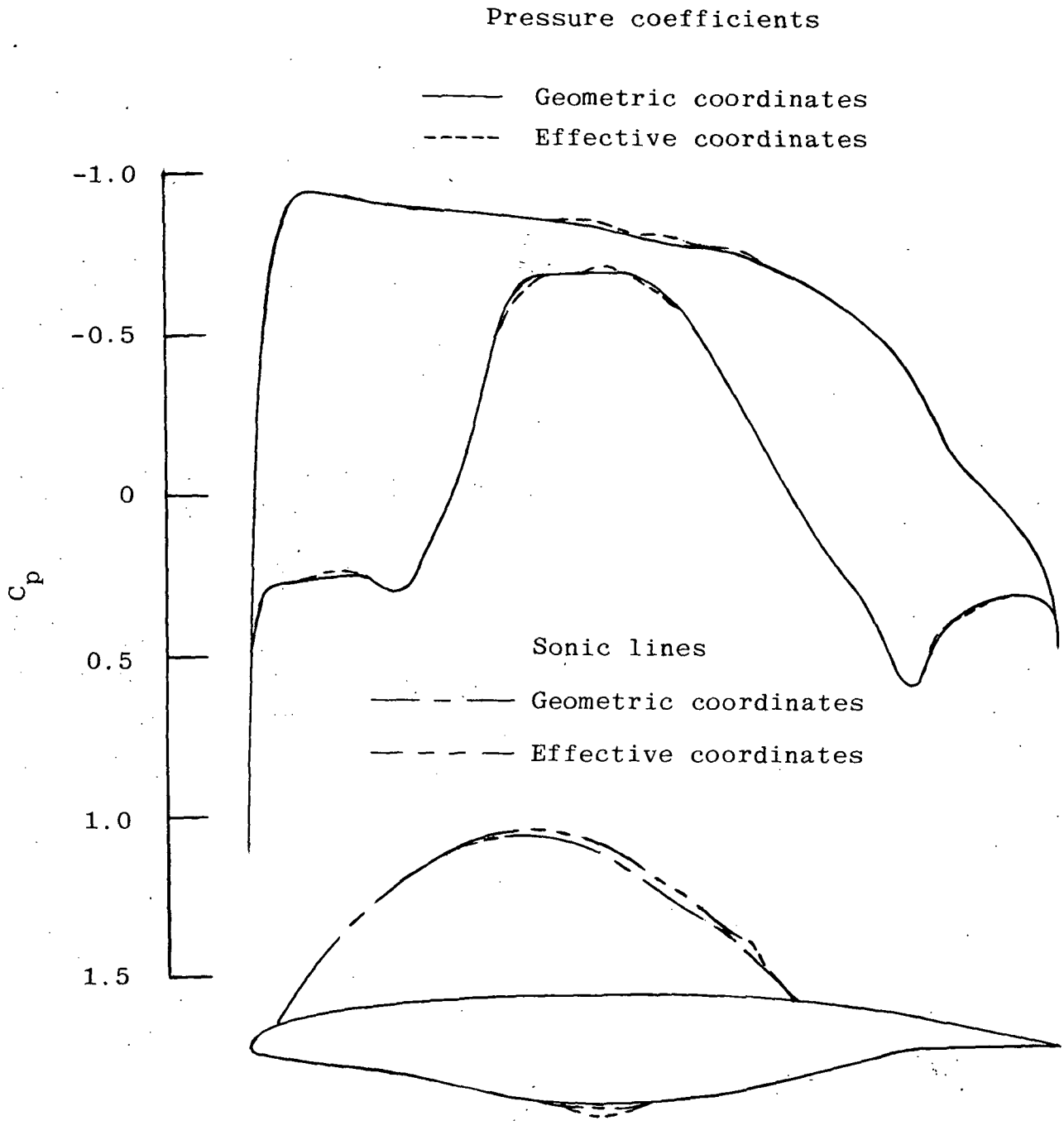


Figure C-4.- 2-D pressure coefficients and sonic line locations for geometric and effective airfoil coordinates for LFC Airfoil YNRB-12-2-77.

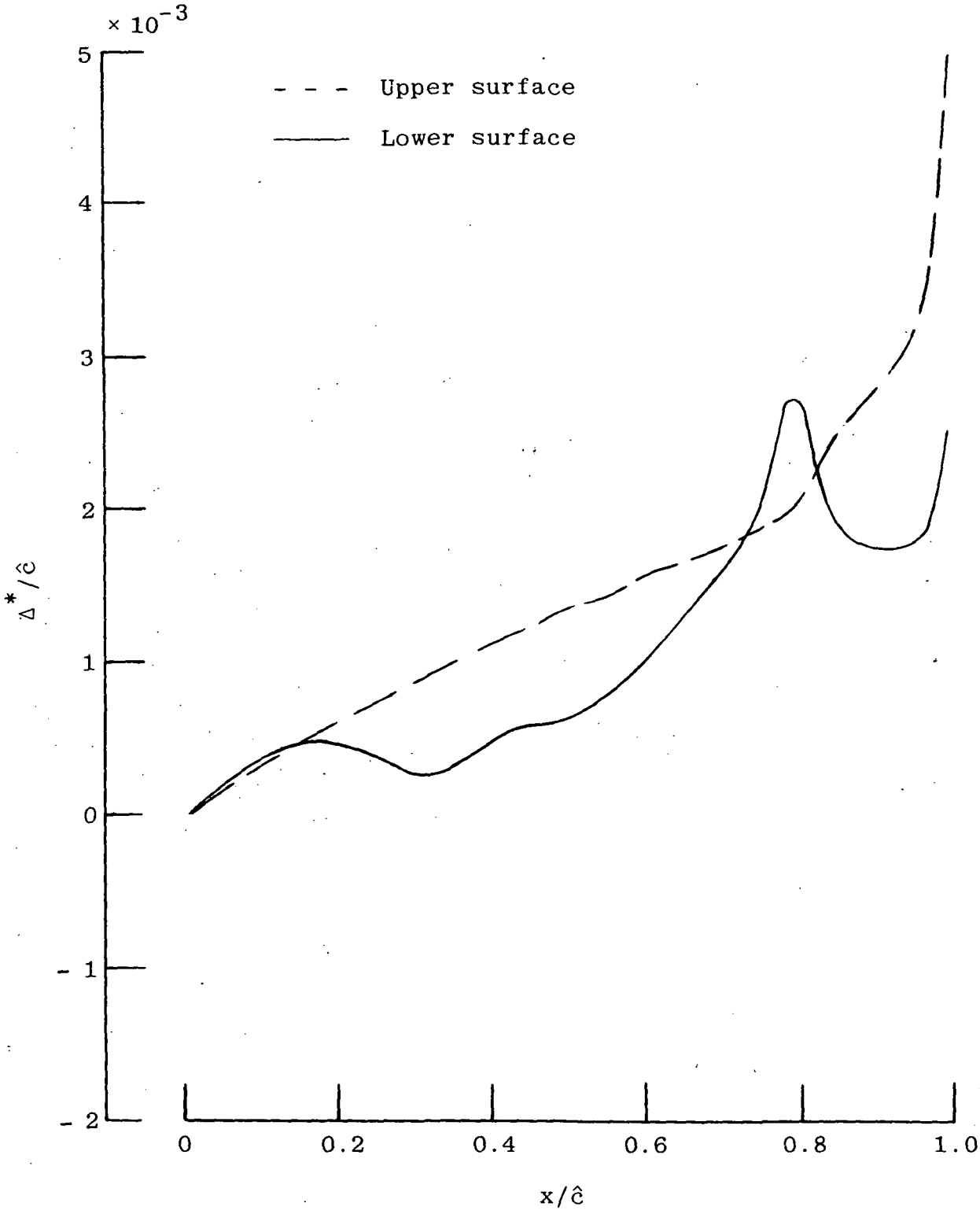


Figure C-5.- Effective displacement-thickness distributions for turbulent flow with laminar flow stability suction rates applied on LFC Airfoil YNRB-12-2-77 at test conditions.

alternate procedure is to determine mass-transfer rate distributions for an effective displacement of zero by an iterative solution of equation (1) and use this solution as a guide to specify mass-transfer rates which result in displacements having a negligible influence on the airfoil performance. The mass-transfer rate distributions for zero $\Delta^*/c$ are presented in figure C-6. For these calculations, convergence was assumed to be $|\Delta^*/c| \leq 10^{-8}$. The rapid growth in CQ near the leading edge is the result of assuming fully developed turbulent flow, and the downstream irregularities reflect changes in the pressure gradient. (See figure C-1.) By inspection of figure C-6, a relative mean constant CQ of $-1.5 \times 10^{-3}$ was selected and applied to both the upper and lower surfaces of the airfoil. The resulting effective displacement thickness distributions are shown in figure C-7. For this airfoil at these test conditions, the constant value of CQ appears to be satisfactory.

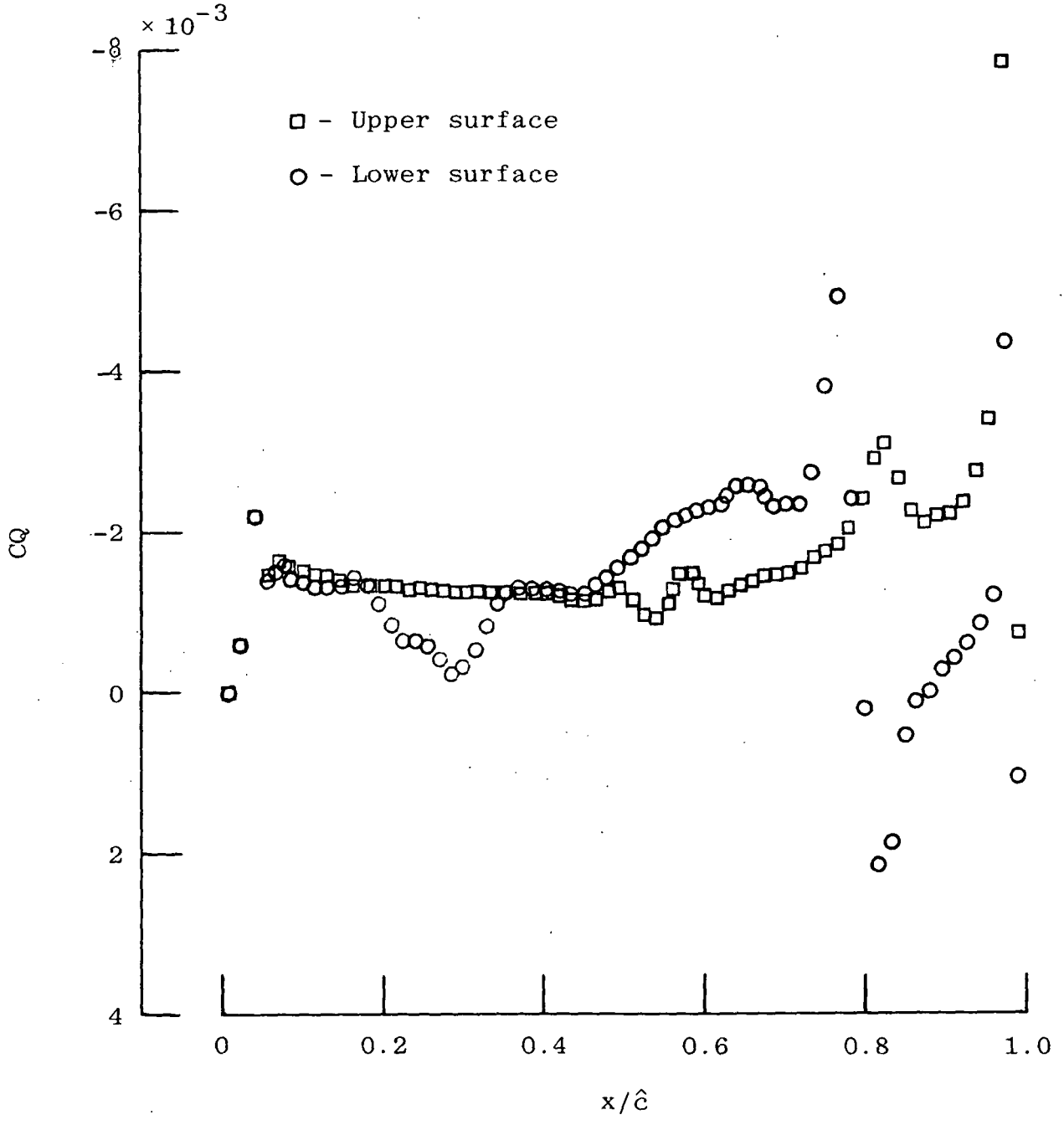


Figure C-6.- Calculated surface mass-transfer rate distributions to maintain zero effective displacement thickness for turbulent flow on LFC Airfoil YNRB-12-2-77 at test conditions.

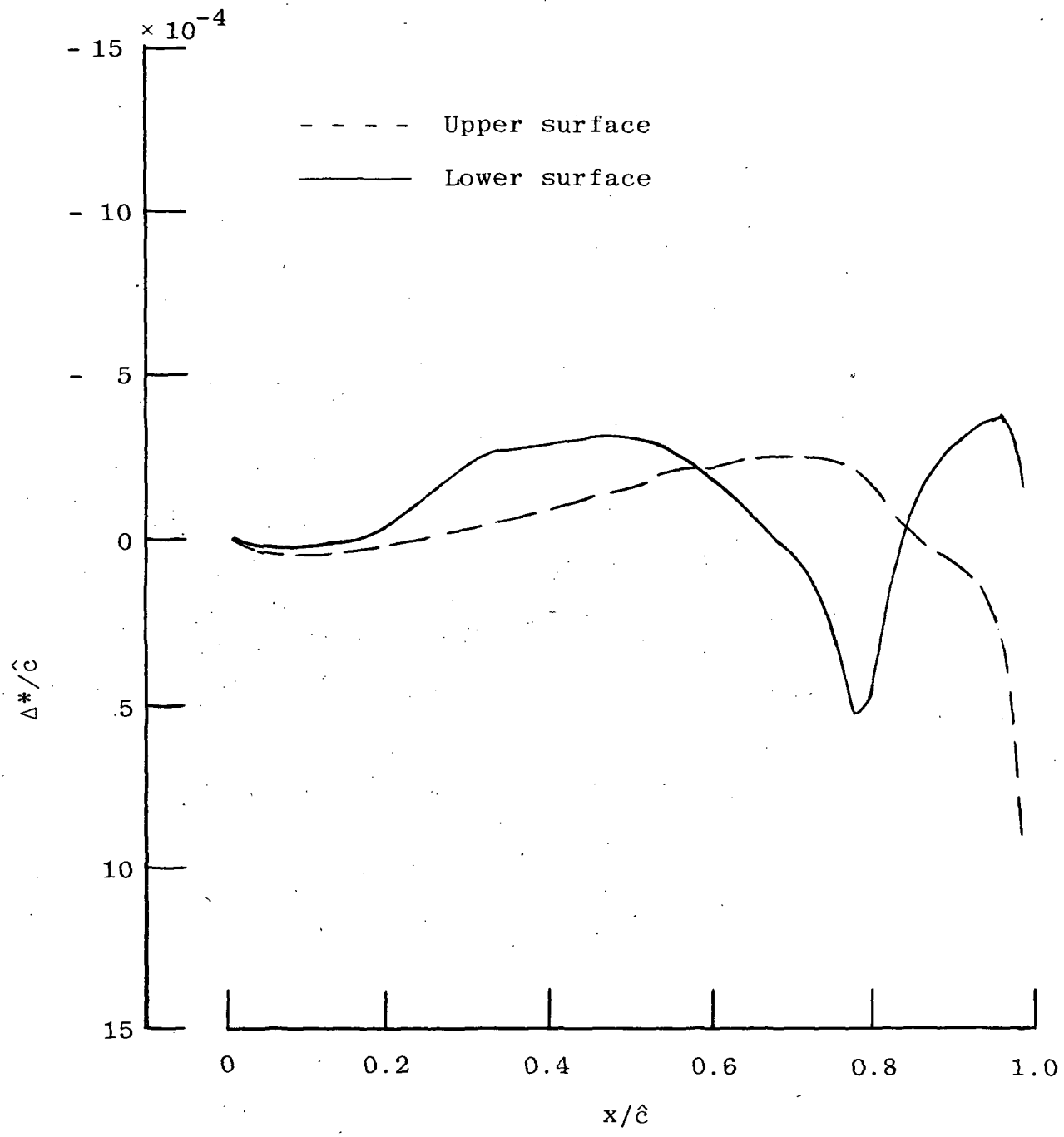


Figure C-7.- Effective displacement-thickness distributions for turbulent flow with a constant suction rate, CQ = - 0.0015, applied on LFC Airfoil YNRB-12-2-77 at test conditions.

## APPENDIX D

## REPRESENTATIVE LINER CALCULATIONS

Some of the computer codes needed for a complete inviscid liner design are currently being developed by NASA. However, the boundary-layer computer code developed for this application has been applied to the streamlines forming the contours of a liner test section for a preliminary LFC airfoil designated as 971T. The velocity-field superpositioning used to obtain the liner contraction section contours (see appendix A) has been bypassed; streamlines and the local flow-field properties along them have been determined for free-air flow about the airfoil at the following conditions:

Freestream Mach number, $M_\infty = 0.82$
Freestream Reynolds number, $N_{Re,\infty} = 26 \times 10^6$, based on the streamwise chord
Stagnation pressure, $P_o = 13$ PSIA
Stagnation temperature, $T_o = 508^\circ$ R
Wing-normal chord, $c = 6.49$ ft.
Streamwise chord $\hat{c} = 7.0$ ft.
Sweep angle, $\Lambda = 22^\circ$

The determination of suction-rate distributions required to maintain an attached boundary layer on the liner sidewalls near the airfoil/liner junction is the only part of the design procedure which is not fully automated. For this part of the analysis, it appears that the most satisfactory method is a cut-and-try approach. That is, one specifies a number of suction-rate distributions along each streamline for which the flow separates in the absence of suction. The computer program monitors the solutions corresponding to suction-rate distributions which result in attached boundary-layer flow, and selects for output the one for which the total mass removed is least. For the present calculations, the suction-rate levels have been restricted to the range $-0.008 \leq CQ \leq 0$ in increments (multiples)

of 0.002; a maximum of three different levels of CQ was considered for a given distribution. However, as many as 10 discontinuous changes in the suction-rate level may be specified in a given distribution, or the distributions may be specified as having a continuous variation.

The suction rates indicated in figure D-1 were obtained by specifying approximately 10 different suction-rate distributions for each of the six streamlines that required suction to maintain attached flow. The figure shows the ordinates of the airfoil and the suction-rate distribution on the liner sidewall near one of the airfoil/liner junctions. The suction rates ahead of the airfoil leading edge are shown to demonstrate that the computer code can be applied successfully to obtain attached boundary-layer solutions in the leading-edge region where the approaching boundary layer is relatively thick. In the LFC experiment, the boundary layer in the leading-edge region will be controlled by the use of much larger suction rates close to the leading edge. It is noted that the flow is three-dimensional in the junction region downstream of the leading edge where suction is applied. The suction-rate distributions specified by a two-dimensional analysis can be considered only as an indication of the rates necessary, and provisions will be included in the suction control system of the experimental facility to vary these rates by a factor of two or more.

A representative liner cross section taken downstream of the airfoil trailing edge is shown in figure D-2. For this liner the entrance cross section is rectangular. The steps in the liner walls result from different spanwise deflections of the streamline that divides and passes through the different flow-field environments above and below the upper and lower surfaces of the swept-wing panel at lift. The streamlines forming the surfaces of these steps originate at different locations along the

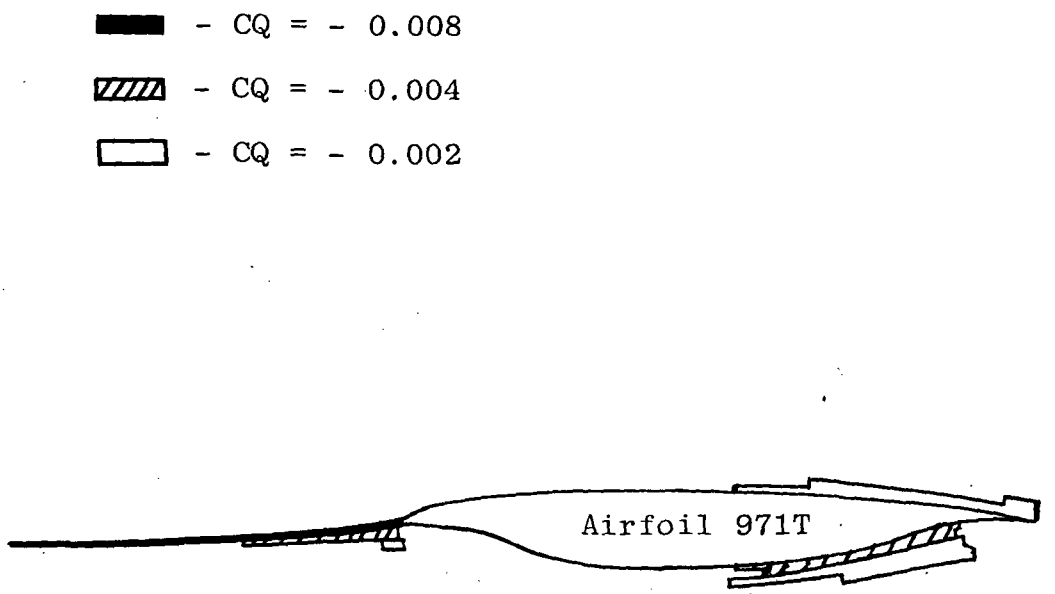


Figure D-1.- Suction rate distributions for attached turbulent boundary layer on contoured liner wall for flow about yawed-wing model.

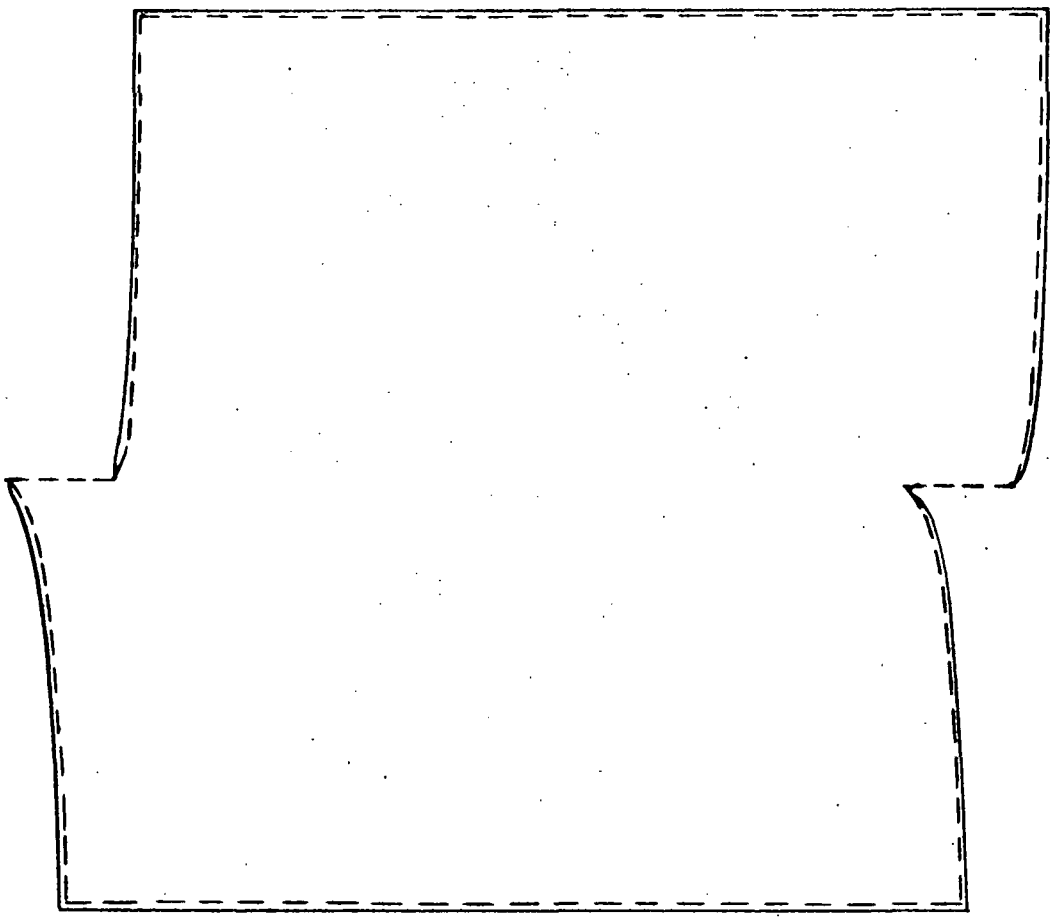

----- Inviscid liner

——— Displacement corrected liner

Figure D-2.- Contoured liner cross section downstream from trailing edge of yawed-wing model.

span of the model at the attachment line instead of at an upstream location on the wall liner. The boundary-layer displacement data are shown only for the streamlines that originate at an upstream location on the wall liner. For the cross section shown in figure D-2, the boundary-layer displacement correction is approximately 3.5 percent of the channel area and is representative of the displacement correction throughout the liner test section. For the high subsonic Mach number considered, the displacement is sufficient to result in choking unless the displacement corrections are made.

Figure D-3 shows the boundary-layer displacement distributions near the airfoil/liner junction and the development of the step on the left liner sidewall at $x/\hat{c}$ = 0, 0.4, 0.8, and 1.2. Suction causes a reduction in the boundary-layer displacement thickness in the immediate vicinity of the airfoil/liner junction; and, at some streamwise locations, the resulting effective displacement corrections are negative.

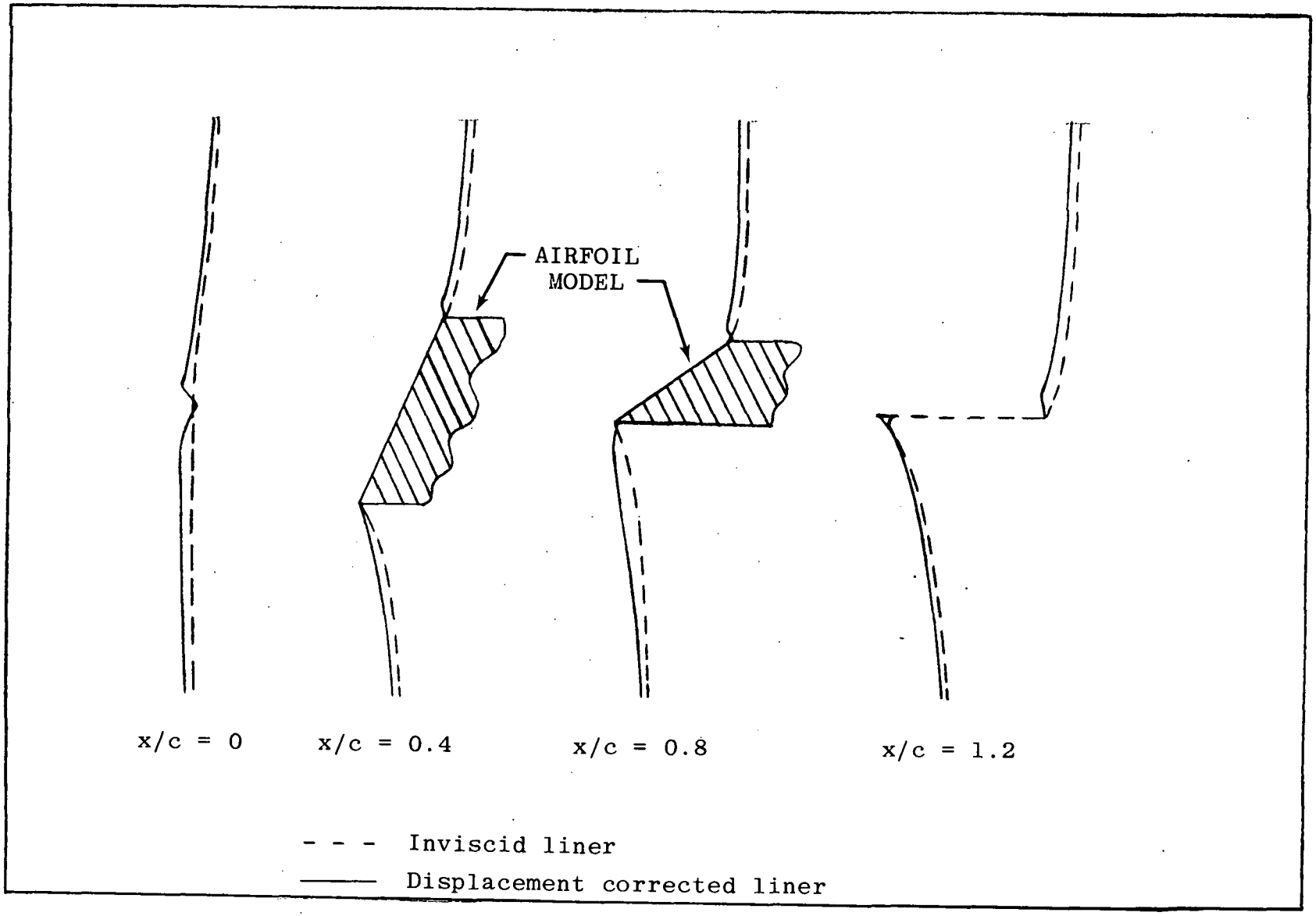


Figure D-3.- Development of liner sidewall contours near airfoil/liner junction for flow about yawed-wing model.

## APPENDIX E

## INVISCID-VISCOUS INTERACTIONS IN WIND TUNNELS

A modification set for the basic boundary-layer computer code LTBPG has been developed for interacting the viscous-displacement correction with the mean inviscid flow field in closed channels. This modification set (program CHANL) was developed in order to analyze the effects of a reduced test section area and/or suction upon subsonic diffuser performance. If there are no shockwave-boundary-layer interactions, the analysis is applicable to supersonic nozzles and wind tunnels.

This program has been applied to analyze the diffuser performance of the NASA Langley 8-foot transonic wind-tunnel facility with a reduced test section area. A reduced test-section area increases the adverse pressure gradients in the diffuser and boundary-layer control may be required to maintain attached flow. The program contains provisions for analyzing the influence of area distributed surface mass transfer upon subsonic diffuser performance. Interacted solutions are obtained by successive approximations using a weighted viscous-displacement geometry and area-ratio relations along with perfect-gas isentropic relations to define the inviscid edge conditions. The iteration procedure is continued until the maximum local change in the Mach number distribution between successive iterations is less than 0.1 percent or until a flow separation is predicted if a subsonic diffuser is being analyzed. For the analysis of subsonic wind-tunnel diffusers, the inviscid edge conditions corresponding to the diffuser's geometric area-ratio distribution generally results in a predicted flow separation if the test section Mach number is above about 0.5 and the diffuser half-angle is greater than about 2.0 degrees. For these cases, an inverse approach to the converged solution or a predicted flow separation is utilized. This procedure requires that the first solution pass be determined using an approximate geometry for which flow separation is not predicted.

Figures E-1 and E-2 present representative results obtained for the Langley 8-foot transonic wind tunnel operating at a Mach number of 0.80 without a test model in place. The stagnation pressure and temperature were 13 PSIA and 508°R, respectively, and the freestream Reynolds number was $4.0 \times 10^6$/foot for the calculations and two runs of the tunnel. The experimental facility was operated at these conditions primarily to determine the noise level in the test section; velocity profile data were measured only at the first diffuser exit. Figure E-1 shows the wind-tunnel geometry from the entrance of the test section to the end of the diffuser and the corresponding computed displacement geometries for two conditions: (a) no mass transfer and (b) a constant suction rate of - 0.001 applied over the interval $56 \leq Z \leq 63$. The boundary-layer calculations were started at the entrance of the wind-tunnel contraction section and transition from laminar to turbulent flow was initiated at the location where the vorticity Reynolds number first exceeded 2800. The behavior of the displacement geometries is as expected both with and without suction. The velocity profile computed for the case of no mass transfer is compared with the two experimentally determined profiles at the diffuser exit, $Z = 131$, in figure E-2. The experimental velocity profile data* were obtained using a pressure scanning probe. A time interval of approximately 20 seconds was required to scan all of the pressure probes used to determine a velocity profile. The agreement between the computed and experimentally determined velocity profiles is only fair. However, the computed boundary-layer thickness and the displacement thickness differ from the experimental values by less than 10 percent. The same test conditions and tunnel geometry were analyzed using the computer code discussed in reference 7 and a flow separation was predicted upstream of the step in the diffuser.

*The wind-tunnel experiments were conducted by Joseph Brooks of NASA Langley Research Center, and the data have not been published. The release of these data is appreciated and acknowledged.

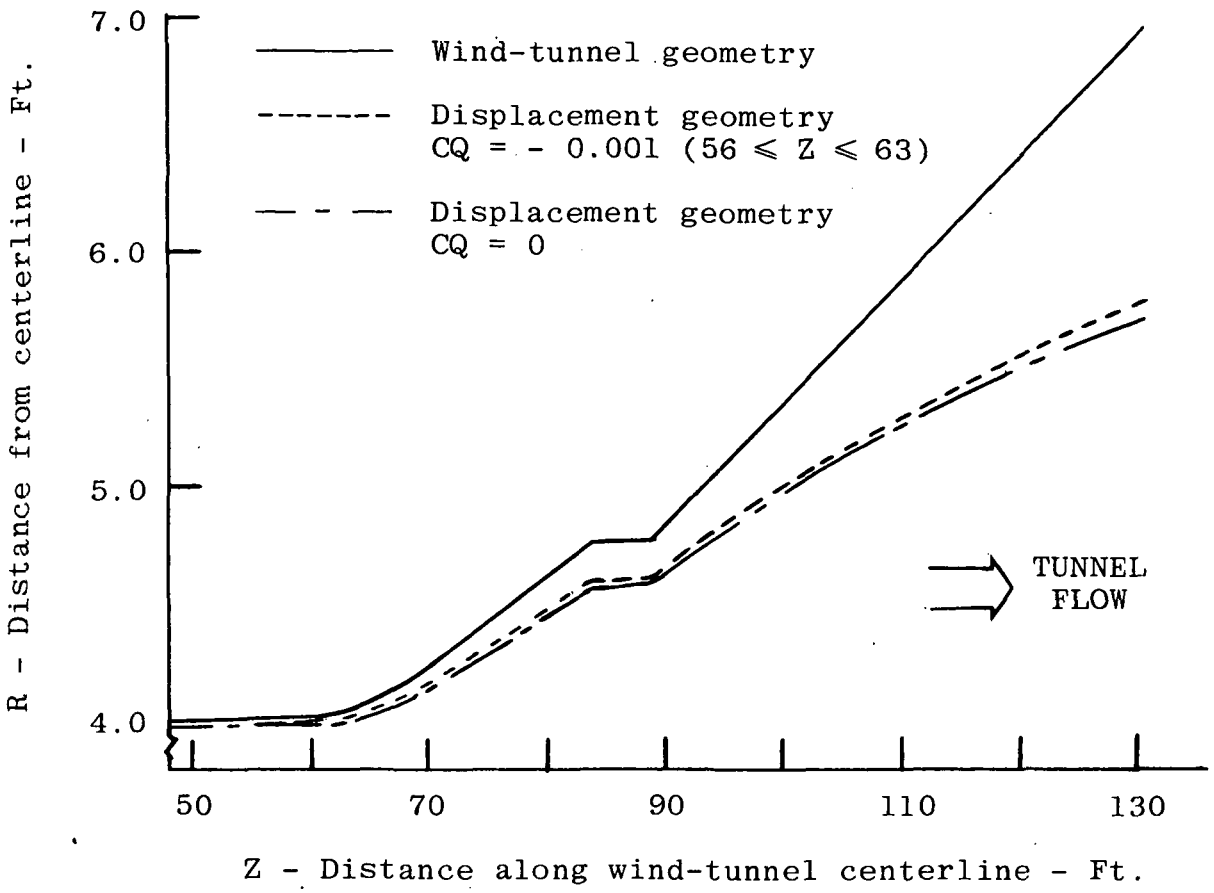


Figure E-1.- Wind-tunnel geometry and effective geometries.

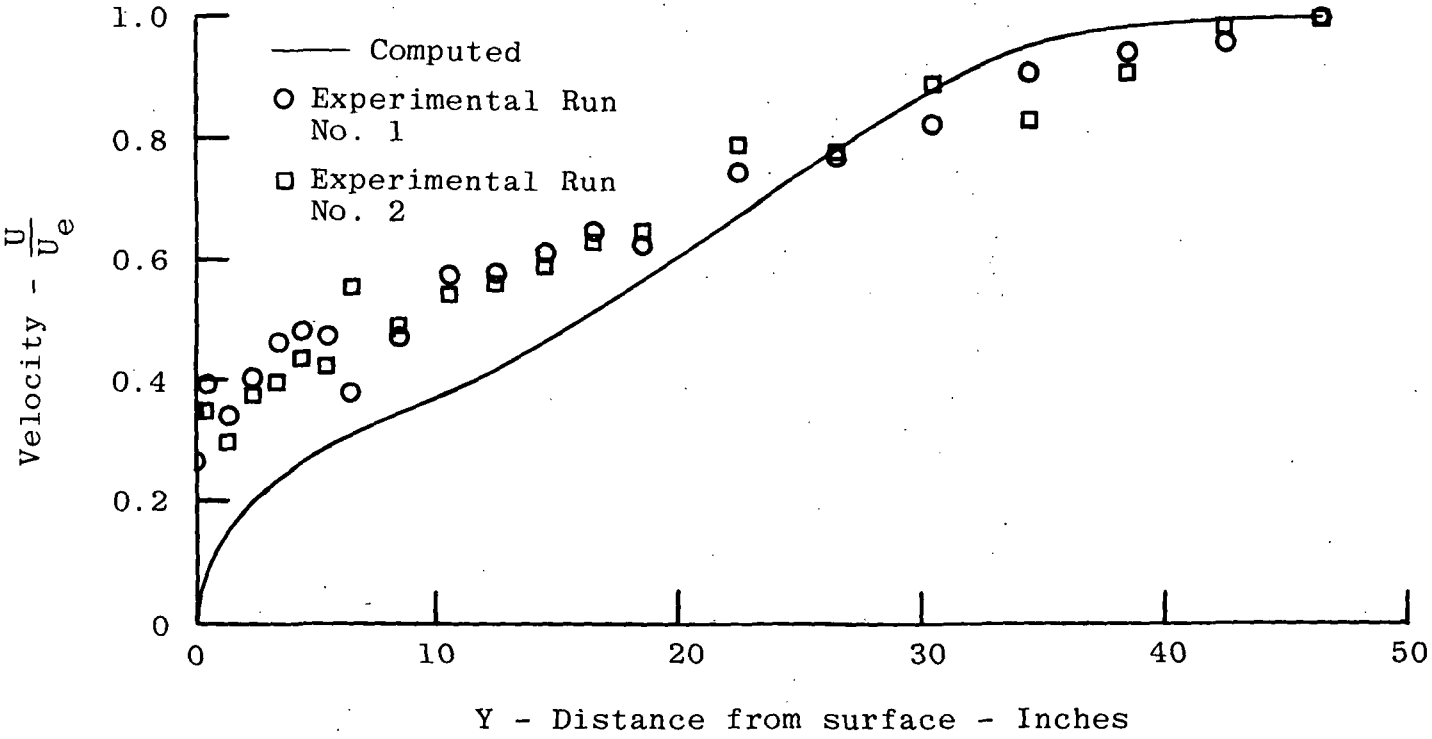


Figure E-2.- Comparison of velocity profiles at tunnel location Z = 131.

The two solution procedures showed excellent agreement with each other up to the entrance of the diffuser. Additional comparisons with more complete experimental data taken at several locations along a diffuser axis are necessary to establish the accuracy of the numerical solution procedures.

Provisions are included in this modification set to permit the analysis of tangential slot injection, and this option has been debugged using an over-simplified turbulence model. A more complete turbulence model has not been included since this method for controlling the boundary layer in the diffuser was considered to be incompatible with the low noise level requirements for laminar flow control experiments.

## REFERENCES


1. Miner, E. W., Anderson, E. C.; and Lewis, Clark H.: A Computer Program for Two-Dimensional and Axisymmetric Nonreacting Perfect Gas and Equilibrium Chemically Reacting Laminar, Transitional, and/or Turbulent Boundary Layer Flows, VPI-E-71-8, May 1971 (Available as NASA CR-132601).

2. Anderson, E. C., and Lewis, C. H.: Laminar or Turbulent Boundary-Layer Flows of Perfect Gases or Reacting Gas Mixtures in Chemical Equilibrium. NASA CR-1893, 1971.

3. Fannelop, T. K.: Displacement Thickness for Boundary Layers with Surface Mass Transfer. AIAA J., Vol. 4, No. 6, June 1966, pp 1142-1144.

4. Goodyer, M. J.: The Self-Streamlining Wind Tunnel. NASA TM X-72699, 1975.

5. Bauer, Frances; Garabedian, Paul; Korn, David; and Jameson, Antony: Supercritical Wing Sections II, Springer-Verlag, New York, 1975.

6. Carlson, Leland A.: TRANDES: A Fortran Program for Transonic Analysis or Design. NASA CR-2821, 1977.

7. Ferguson, D. R.: and Keith, J. S.: Modifications to the Streamtube Curvature Program. Volume 1. Program Modifications and user's manual. NASA CR-132705, 1975.

8. Newman, P. A.; and Anderson, E. C.: Numerical Design of Streamlined Tunnel Walls for a Two-Dimensional Transonic Test. NASA TM-78641, 1978.

9. Ladson, Charles L.: Description and Calibration of the Langley 6- by 19-Inch Transonic Tunnel. NASA TN D-7128, 1973.

10. Allison, D. O.; and Dagenhart, J. R.: Design of a Laminar-Flow-Control Supercritical Airfoil for a Swept Wing. CTOL Transport Technology-1978. Part 1. NASA CP-2036, 1978, pp 395-408.